Effect of Different Shapes of Nanoparticles on Mixed Convective Nanofluid Flow in a Darcy-Forchhiemer Porous Medium

Annapurna T[1], K. S. R. Sridhar[2], M. Karuna Prasad[1,*]

[1] Department of Mathematics, Ballari Institute of Technology and Management, Ballari-583104, Karnataka India
[2] Department of Mathematics, Kishkinda University, Ballari-583104, Karnataka India

ARTICLE INFO

ABSTRACT

The nanofluid has diverse applications in industries, engineering, and medicine due to its greater thermal characteristics. However, various factors such as the shape and size of nanoparticles, the base fluid, the porous medium, the quadratic drag force, and the viscous dissipation have significant effects on the flow and heat transfer characteristics of nanofluids. Therefore, it is crucial to study the influence of these factors. In this paper, a theoretical investigation is conducted to analyze the mechanisms of thermal conductivities of different shapes of nanoparticles, such as platelet, cylinder, brick and blade on the mixed convective nanofluid flow in a vertical channel saturated with porous medium. Consider ethylene glycol and water as base fluids for the nanoparticles, including copper, aluminum oxide, titanium oxide, silver, and iron oxide. A thin, movable baffle plate of negligible thickness is inserted in the channel and made into double passages. To define the porous matrix, the Darcy-Brinkaman-Forchhiemer model is used, and to define the nanofluid, the Tiwari and Das model is used. Robin boundary conditions are considered for the channel flow. The differential transform method (DTM) is applied to solve non-linear governing equations with inertia, and the perturbation method is applied to solve the problem without inertia. Velocity and temperature cantors are shown graphically using MATLAB and MATHEMATICA. The obtained values by DTM and the perturbation method are well validated and shown graphically. The Nusselt number was evaluated and tabulated for all governing parameters. The objective of this article is to investigate the effect of nonspherical shapes of nanoparticles, the base fluid, the inertial forces of the porous medium, and the buoyancy force on the thermal characteristics of flow and heat transfer of nanofluids. The main findings of this problem are that the optimum velocity and temperature cantor are found for platelet-shaped water-based silver nanofluid.

---

* *Corresponding author.*
E-mail address: karunaprasad9@gmail.com (M. Karuna Prasad)

1. Introduction

The field of nanoscience has burgeoned significantly in the last few decades, and researchers are gradually investigating more fields of application without interruption. Nanotechnology is a scientific method to composite particles in the nanoscale range, from 1 to 100 nm. Its stupendous applications include nuclear reactors, the thermal industry, powder technology, the biomedical industry, etc. The blend of nanoparticles floating in a base fluid (water, oil, ethylene glycol, etc.) is called a nanofluid. Choi and Eastman [1] found that heat transfer capacities and deferment strength are greatly improved when a suspended nanoparticle is used, such as in residential refrigerator freezers, enhancing diesel generator efficiency, boosting chiller heat transfer efficiency, cooling of electronics and transformer oil, solar water heating, nuclear reactors, military and space, cooling of heat exchanging devices, and so on. These particles, also known as nanoparticles, have a diameter of less than 100 nm. Pak and Cho [2] experimentally examined the heat transfer and turbulent friction nature of ultrafine metallic oxide-suspended water flowing through a circular tube. A method for measuring the thermal conductivity of oxide nanofluids was developed by Lee [3]. The results they verified showed that the thermal conductivity of the nanofluid depends not only on the shape of the nanoparticles [4] but also on their size [5, 6].

Nanofluid flows are captured in much mathematical geometry. Such flows could be laminar or turbulent. Fluid dynamics has so many applications in the lubrication industries, gas turbine power plants, polymer technology, food processing industries, plasma power plants, thermal and insulating engineering, MHD power generators, etc. These fluid flows are driven either by natural, forced, or mixed convection. Studied combined forced and natural convective heat transfer and examined mixed convective flow in a vertical tube filled with porous material. Base fluids consist of water, oil, ethylene glycol, and lubricants, which significantly limit heat transfer performance. Nanofluids combine high-quality thermal conductivity with a lower density to facilitate convective heat transfer in a range of applications. The thermal conductivity and fluid mixtures were discussed by Hasan *et al.*, [7, 8]. Properties like viscosity and specific heat have altered dramatically in the basic fluid. Many writers were drawn to work on engineering applications because of these qualities. Numerous researchers have experimented with the common uses of nanofluids, as documented in their literature [9–16].

Another factor that affects the thermal conductivity of nanofluids is the form and shape of nanoparticles [17]. The thermal conductivity of several metallic oxide nanofluids, including CuO/water, ZnO/water, and SiO2/water, was measured by Alawi *et al.*, [18]. Chon *et al.*, [19] have shown that the size of the particles affects the thermal conductivity of Al2O3 nanofluid. Thermal characteristics are superior to standard ones, according to a survey found in the literature [20, 21]. According to existing data, solids have a higher heat conductivity than liquids. Water and motor oil have thousands of times less heat conductivity than copper (Cu). A forced convective nanofluid (Cu-H2O) flow around a solid circular cylinder in an unstable regime was computationally simulated by Yacine *et al.*, [22]. An increase in the concentration of nanoparticles in the base fluid was seen to correspond with an increase in the mean and average Nusselt numbers. The primary energy systems for which TiO2 nanofluids are used are solar collectors and heat pipes. By using certain impurities as base fluids, the thermal conductivity of TiO2 nanofluids can be varied and improved. Karuna Prasad *et al.*, [23, 24] found a higher rate of heat transport in ternary hybrid nanofluid compared to normal fluid in the study of nonlinear thermal convective heat transfer.

Hybrid nanofluids are superior nanofluids than nanofluids. These different combinations of nanoparticles with traditional base fluid exhibit remarkable capabilities in heat transport and hence find applications in nuclear system cooling, heat exchangers, and solar systems [25, 26]. The authors

[27, 28] studied TiO2 and Fe3O4 nanoparticles due to their wide applications in the environment. The numerical investigation of the flow of water-based nanofluid is conducted by Sabeel *et al.*, [29]. He concluded that a high rate of heat transfer occurred for CuO nanoparticles compared to Al2O3 and TiO2 nanoparticles. The effect of MHD on Maxwell micropolar fluid flow is studied by Sabeel *et al.*, [30]. He observed in his results that the increase in the micro-inertial parameter enhanced the flow and suppressed the temperature field. The influence of MHD on viscoelastic fluid flow is studied numerically by Sabeel *et al.*, [31]. He found in his results that the rate of heat transfer and mass transfer decreased with the increase in magnetic field. Taimoor Dil *et al.*, [32] analysed the characteristics of heat transfer with water-based nanofluid. In this study, three different types of nanoparticles are used. Sabeel *et al.*, [33] applied the Galerkin-Petrov finite element method to study the flow and heat transfer of hybrid nanofluid. By increasing the nanoparticle concentration, the rate of heat transfer can be enhanced at both plates. Noorehan Awang *et al.*, [34] used different shapes of nanoparticles in hybrid nanofluid flow. The optimal rate of heat and mass transfer is found in blade-shaped nanoparticles. Nadhira Azreen Azmi *et al.*, [35] found the optimal rate of heat transfer for platelets, followed by cylindrical, brick, and spherical-shaped nanoparticles. Asif Memon *et al.*, [36, 37] observed that the Forchhieimer resistance decreases the temperature profile in the study of flow and heat transfer of nanofluid. Asif Memon *et al.*, [38] found that the velocity decreased with the enhancement in inertial force.

The aim of this work is to carry out a theoretical investigation on the effects of different shapes of nanoparticles on mixed convective flow in a vertical channel saturated with porous media. The several nanofluids with different base fluids in the flow are considered to be under the influence of buoyancy forces. A thin, flat plate is inserted into the channel, making a double-passage channel. The plate is movable and has negligible thickness. The analytical method (using perturbation) and the semi-analytical method (using DTM) are used to solve the governing highly nonlinear equations with Robin boundary conditions [39–41]. The use of porous media and nanofluids are two techniques for enhancing heat transfer that were coupled in the current study. In addition, the effects of inertial force and viscous dissipation were considered. Expressions for the values of the Nusselt number and profiles of temperature and velocity are produced. The thermal conductivity of conventional heat-transfer fluids, such as oil, water, and ethylene glycol mixtures, is known to have a significant impact on the heat-transfer coefficients between the heat-transfer medium and the heat-transfer surface, leading to poor heat-transfer performances. The goal of this effort was to create an innovation in heat transfer in mixed convective flow by inserting a thin flat plate in an open-ended vertical channel and to find uses for it in heat exchangers.

2. Methodology
2.1 Formation of the Problem

Consider an open-ended vertical channel divided by a thin, movable plate of negligible thickness saturated with porous medium (see Figure 1). Analysed the steady, laminar, fully developed flow of nanofluid. The X axis is taken upwards and parallel to the flat wall. The Y axis is taken perpendicular to the X axis, and the plate position is taken as y*. The width of the channel is D.

The origin of the axes is such that the channel walls are in positions y=-h and y=h. For fully developed flow, it is assumed that the transverse velocity is zero and the pressure depends only on x [42]. The fluid is a water-based and ethylene glycol-based nanofluid containing five different types of nanoparticles: copper, aluminium oxide, titanium oxide, silver, and iron oxide. It is assumed that the base fluid and the suspended nanoparticles are in thermal equilibrium.
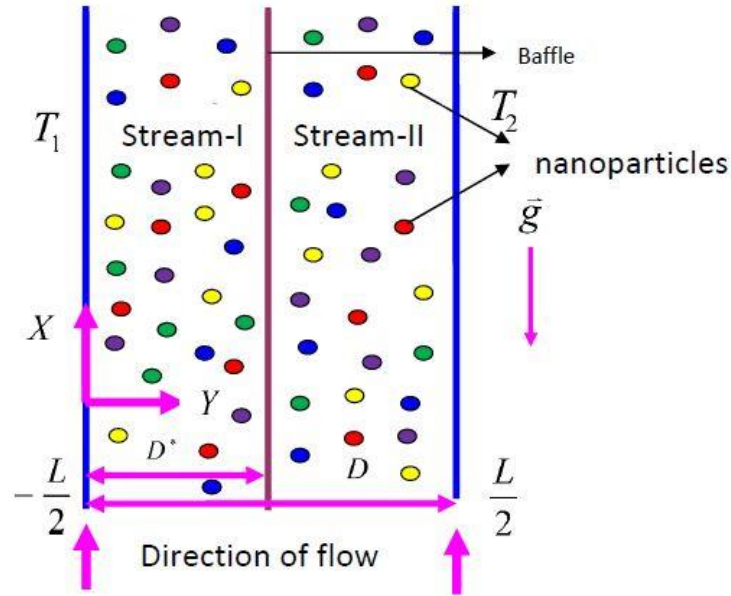
Fig. 1. Physical configuration

Considered U_1 and U_2 are the velocities in stream-I and Stream-II, T_1 and T_2 are the temperatures at left wall and right wall, h_1 and h_2 are the width of the stream-I and stream-II.

The momentum and energy equations for both stream-I and stream-II are

Stream-I

$$(\rho\beta)_{nf}\, g(T_1 - T_0) - \frac{\partial p}{\partial x} + \mu_{nf}\,\frac{d^2 U_1}{dY^2} - \frac{\mu_{nf}}{\kappa} U_1 - \frac{\rho_{nf} C_f}{\sqrt{\kappa}} U_1^{\;2} = 0 \tag{1}$$

$$\frac{\partial^2 T_1}{\partial Y^2} = -\frac{\mu_{nf}}{k_{nf}}\left(\frac{dU_1}{dY}\right)^2 - \frac{\mu_{nf}}{k_{nf}}\frac{U_1^{\;2}}{\kappa} \tag{2}$$

Stream-II

$$(\rho\beta)_{nf}\, g(T_2 - T_0) - \frac{\partial p}{\partial x} + \mu_{nf}\,\frac{d^2 U_2}{dY^2} - \frac{\mu_{nf}}{\kappa} U_2 - \frac{\rho_{nf} C_f}{\sqrt{\kappa}} U_2^{\;2} = 0 \tag{3}$$

$$\frac{\partial^2 T_2}{\partial Y^2} = -\frac{\mu_{nf}}{k_{nf}}\left(\frac{dU_2}{dY}\right)^2 - \frac{\mu_{nf}}{k_{nf}}\frac{U_2^{\;2}}{\kappa} \tag{4}$$

Where μ_{nf} is the viscosity of the nanofluid, ρ_{nf} the density of the nanofluid, β_{nf} the coefficient of thermal expansion of the nanofluid, k_{nf} the thermal conductivity of the nanofluid, which are given by

$$\mu_{nf} = \mu_f \left(1 + a1\phi + b1\phi^2\right), \quad \rho_{nf} = (1-\phi)\rho_f + \rho_s\phi, \qquad (\rho\beta)_{nf} = \rho_{nf}\beta_{nf} = (1-\phi)(\rho\beta)_f + (\rho\beta)_s\phi \qquad \text{and}$$

$$k_{nf} = k_f \left[\frac{k_s + (n-1)k_f - (n-1)\phi(k_f - k_s)}{k_s + (n-1)k_f + \phi(k_f - k_s)} \right]$$

Where ϕ is the nanoparticle volume fraction, μ_f is the viscosity of the base-fluid, ρ_f the density of the base-fluid, β_f the coefficient of thermal expansion of the base-fluid, k_f the thermal conductivity of the base-fluid, μ_s is the viscosity of the solid particle, ρ_s the density of the solid particle, β_s the coefficient of thermal expansion of the solid particle, k_s the thermal conductivity of the solid particle.

The empirical shape factor is given by $n = \frac{3}{\psi}$ where ψ is the sphericity defined as the ratio between the surface area of the sphere and the surface area of the real particle with equal volumes. The values of ψ for different shapes of particles are given in Table 1.

Table 1
Sphericity Ψ for different shapes of nanoparticles [43]

Model	Platelet	Blade	Cylinder	Brick
Ψ	0.52	0.36	0.62	0.81

Let a and b are constants depend on the particle shapes are given in Table 2.

Table 2
Constants a1 and b1 empirical factors [43]

Model	Platelet	Blade	Cylinder	Brick
a1	37.1	14.6	13.5	1.9
b1	612.6	123.3	904.4	471.4

The boundary, interface conditions on velocity, temperature cantors are

$$U_1 = 0, T_1 = T_0, \quad \text{at } Y = -h$$

$$U_2 = 0, T_2 = T_0, \text{ at } Y = h$$

$$U_1 = U_2 = 0, T_1 = T_2, \quad \frac{dT_1}{dY} = \frac{dT_2}{dY}, \quad \text{at } Y = y^* \tag{5}$$

Where y^* is a position of the plate. The thermophysical properties of base fluid and particles are given in Table 3.

Table 3
Thermophysical properties of base fluid and particles [43]

Model	$\rho\left(kgm^{-3}\right)$	$c_p\left(kg^{-1}K^{-1}\right)$	$k(Wm^{-1}K^{-1})$	$\beta\times10^{-5}\left(K^{-1}\right)$
H_2O	997.1	4179	0.613	21
$C_2H_6O_2$	1.115	0.58	0.1490	6.5
Cu	8933	385	401	1.67
TiO_2	4250	686.2	8.9528	0.9
Ag	10500	235	429	1.89
Al_2O_3	3970	765	40	0.85
Fe_3O_4	5180	670	9.7	0.5

Introducing non-dimensional parameters in the governing equations of momentum and energy such as

$$u_i = \frac{U_i}{U_0}, \qquad y = \frac{Y}{D}, \qquad R_T = \frac{T_2-T_1}{\Delta T}, \quad s = \frac{Bi_1 Bi_2}{Bi_1 Bi_2 + 2 Bi_1 + 2 Bi_2}, \qquad Br = \frac{\mu_f U_0^2}{k_f \Delta T}, \qquad \text{Re} = \frac{U_0 D\rho_f}{\mu_f},$$

$$Gr = \frac{\beta_f g\Delta T D^3}{v_f^2}, \quad \sigma = \frac{D}{\sqrt{\kappa}}, \quad \delta = \frac{\rho_f C_f U_0 D^2}{\sqrt{\kappa}\mu_f}, \quad v_f = \frac{\mu_f}{\rho_f}, \quad Bi_2 = \frac{h_2 D}{k_f}, \quad Bi_1 = \frac{h_1 D}{k_f}, \quad \Lambda = \frac{Gr}{\text{Re}} \qquad (6)$$

where Br is Brinkman number, Re is Reynold's number, Gr is Grashoff number, σ porous parameter, δ inertial parameter, v_f is kinematic viscosity of the base fluid, Bi_1 and Bi_2 are Biot numbers and Λ is mixed convection parameter.

Assumed isothermal wall temperatures for the channel. In particular, the boundary temperature at $Y = -h_1/2$ is T_1, while the boundary temperature at $Y = h_2/2$ is T_2 with $T_2 > T_1$. These boundary conditions are compatible with Eq. (1) and (3) if and only if dP/dX is independent of X. Therefore, the pressure gradient is considered as a constant.

$$\frac{dp}{dX} = A \qquad (7)$$

The reference velocity and temperature are given by Ref. [38]

$$U_0 = -\frac{AD^2}{48\mu_f} \text{ and } T_0 = \frac{T_1+T_2}{2} + S\left(\frac{1}{Bi_1} - \frac{1}{Bi_2}\right)(T_2 - T_1). \qquad (8)$$

One obtains the combined momentum and energy equations using non-dimensional parameters corresponding to streams I and II as

Stream-I

$$\frac{d^4u_1}{dy^4} = \sigma^2 \frac{d^2u_1}{dy^2} + E_1E_3 I \frac{d^2u_1^2}{dy^2} + \frac{E_1E_2}{E_4}\sigma^2 \Lambda Br\, u_1^2 + \frac{E_1E_2}{E_4}\Lambda Br\left(\frac{du_1}{dy}\right)^2 \qquad (9)$$

Stream-II

$$\frac{d^4 u_2}{dy^4} = \sigma^2 \frac{d^2 u_2}{dy^2} + E_1 E_3 I \frac{d^2 u_2^2}{dy^2} + \frac{E_1 E_2}{E_4} \sigma^2 \Lambda B r u_2^2 + \frac{E_1 E_2}{E_4} \Lambda B r \left(\frac{du_2}{dy} \right)^2 \tag{10}$$

Subject to the boundary conditions for both streams I and II

$$u_1 = 0 \text{ at } y = -\frac{1}{4} \text{ and } u_2 = 0 \text{ at } y = \frac{1}{4}$$

$$\frac{1}{Bi_1} \frac{d^3 u_1}{dy^3} - \frac{1}{E_4} \frac{d^2 u_1}{dy^2} - \frac{\sigma^2}{Bi_1} \frac{du_1}{dy} = Bc_3, \quad \text{at } y = -\frac{1}{4}$$

$$\frac{1}{Bi_2} \frac{d^3 u_2}{dy^3} + \frac{1}{E_4} \frac{d^2 u_2}{dy^2} - \frac{\sigma^2}{Bi_2} \frac{du_2}{dy} = Bc_4, \quad \text{at } y = \frac{1}{4}$$

$$u_1 = 0, \; u_2 = 0 \text{ at } y = y*$$

$$\frac{d^2 u_1}{dy^2} = \frac{d^2 u_2}{dy^2} \quad at \; y = y*,$$

$$\frac{d^3 u_1}{dy^3} - \sigma^2 \frac{du_1}{dy} = \frac{d^3 u_2}{dy^3} - \sigma^2 \frac{du_2}{dy} \quad at \quad y = y* \tag{11}$$

where $E_1 = \frac{\mu_{nf}}{\mu_f}$, $E_2 = \frac{(\rho\beta)_{nf}}{(\rho\beta)_f}$, $E_3 = \frac{\rho_{nf}}{\rho_f}$, $E_4 = \frac{k_{nf}}{k_f}$,

2.2 Perturbation Method

The obtained governing Eq. (9) and Eq. (10) are highly nonlinear and are solved by the perturbation method without inertia term. The solutions are found using the perturbation method. The perturbation method can strongly justify with a small value of perturbation parameter ε ($\varepsilon = \Lambda B r$).

$$u_i(y) = u_{i0}(y) + \varepsilon u_{i1}(y) + \varepsilon^2 u_{i2}(y) + \dots \tag{12}$$

Substituting Eq. (12) in Eq. (9), Eq. (10), and Eq. (11) and equating the coefficients of ε to obtain zeroth and first order equations.

Zeroth order equations

$$\frac{d^4 u_{10}}{dy^4} = \sigma^2 \frac{d^2 u_{10}}{dy^2} \tag{13}$$

First order equations

$$\frac{d^4 u_{11}}{dy^4} = \sigma^2 \frac{d^2 u_{11}}{dy^2} + \frac{E_1 E_2}{E_4} \sigma^2 u_{10}{}^2 + \frac{E_1 E_2}{E_4} \left(\frac{du_{10}}{dy} \right)^2 \tag{14}$$

Stream-II

Zeroth order equations

$$\frac{d^4 u_{20}}{dy^4} = \sigma^2 \frac{d^2 u_{20}}{dy^2} \tag{15}$$

First order equations

$$\frac{d^4 u_{21}}{dy^4} = \sigma^2 \frac{d^2 u_{21}}{dy^2} + \frac{E_1 E_2}{E_4} \sigma^2 u_{10}{}^2 + \frac{E_1 E_2}{E_4} \left(\frac{du_{20}}{dy} \right)^2 \tag{16}$$

The boundary, interface conditions for both streams I and II are

Zeroth order

$$u_{10} = 0 \ \text{ at } \ y = -\frac{1}{4}, \quad u_{20} = 0 \ \text{ at } \ y = \frac{1}{4},$$

$$\frac{1}{Bi_1} \frac{d^3 u_{10}}{dy^3} - \frac{1}{E_4} \frac{d^2 u_{10}}{dy^2} - \frac{\sigma^2}{Bi_1} \frac{du_{10}}{dy} = Bc_3, \quad \text{at } \ y = -\frac{1}{4}$$

$$\frac{1}{Bi_2} \frac{d^3 u_{20}}{dy^3} + \frac{1}{E_4} \frac{d^2 u_{20}}{dy^2} - \frac{\sigma^2}{Bi_2} \frac{du_{20}}{dy} = Bc_4 \quad \text{at } \ y = \frac{1}{4}$$

$$u_{10} = 0, \ u_{20} = 0 \ \text{at} \ y = y*$$

$$\frac{d^2 u_{10}}{dy^2} = \frac{d^2 u_{20}}{dy^2} \ \text{at} \ y = y*,$$

$$\frac{d^3 u_{10}}{dy^3} - \sigma^2 \frac{du_{10}}{dy} = \frac{d^3 u_{20}}{dy^3} - \sigma^2 \frac{du_{20}}{dy} \ \text{at} \ y = y^* \tag{17}$$

First order

$$u_{11} = 0 \ \text{ at } \ y = -\frac{1}{4}, \quad u_{21} = 0 \ \text{ at } \ y = \frac{1}{4},$$

$$\frac{1}{Bi_1}\frac{d^3u_{11}}{dy^3} - \frac{1}{E_4}\frac{d^2u_{11}}{dy^2} - \frac{\sigma^2}{Bi_1}\frac{du_{11}}{dy} = 0, \quad \text{at } y = -\frac{1}{4}$$

$$\frac{1}{Bi_2}\frac{d^3u_{21}}{dy^3} + \frac{1}{E_4}\frac{d^2u_{21}}{dy^2} - \frac{\sigma^2}{Bi_2}\frac{du_{21}}{dy} = 0 \quad \text{at } y = \frac{1}{4}$$

$$u_{11} = 0, \ u_{21} = 0 \text{ at } y = y*$$

$$\frac{d^2u_{11}}{dy^2} = \frac{d^2u_{21}}{dy^2} \text{ at } y = y*,$$

$$\frac{d^3u_{11}}{dy^3} - \sigma^2\frac{du_{11}}{dy} = \frac{d^3u_{21}}{dy^3} - \sigma^2\frac{du_{21}}{dy} \quad \text{at } y = y* \tag{18}$$

The solutions obtained for zeroth and first order Eq. (13) to Eq. (16) using the conditions Eq. (17) and Eq. (18) are given as

Zeroth order solutions

Stream-I

$$u_{10} = d_1 + d_2y + d_3Cosh[\sigma y] + d_4Sinh[\sigma y] \tag{19}$$

Stream-II

$$u_{20} = d_5 + d_6y + d_7Cosh[\sigma y] + d_8Sinh[\sigma y] \tag{20}$$

First order solutions

Stream-I

$$u_{11} = c_3 + c_4y + k_{10}y^2 + k_{11}y^3 + k_{01}y^4 + k_{12}Cosh(\sigma y) + k_{13}Sinh(\sigma y) + k_{14}yCosh(\sigma y)$$
$$+ k_{15}ySinh(\sigma y) + k_{16}y^2Cosh(\sigma y) + k_{17}y^2Sinh(\sigma y) + k_{18}Cosh(2\sigma y) + k_{19}Sinh(2\sigma y) \tag{21}$$

Stream-II

$$u_{21} = H_{13} + H_{14}y + H_{15}Cosh[B_1 y] + H_{16}Sinh[B_1 y] + k_{30}Cosh[2B_1 y] + k_{31}Sinh[2B_1 y] +$$
$$k_{32}yCosh[B_1 y] + k_{33}ySinh[B_1 y] + k_{34}y^2Cosh[B_1 y] + k_{35}y^2Sinh[B_1 y] + k_{36}y^4 + k_{37}y^3 + k_{38}y^2 \tag{22}$$

Too many constants are there and hence not shown in the paper.

2.3 Differential Transform Method

The obtained governing Eq. (9) and Eq. (10) are highly nonlinear differential equations and are solved with inertial by using differential transform method.

The DTM method was introduced by Ref. [39] who solved electric circuit analysis problems. Taylor series expansion is used to construct this method and is a semi-analytical numerical technique.

The kth derivative differential transforms of the $f(y)$ is defined as follows:

$$F[k] = \frac{1}{k!}\left[\frac{d^k f(y)}{dy^k}\right]_{y=y_0} \tag{23}$$

where $f(y)$ is the given function and $F[k]$ is transformed function. Differential inverse transforms of $F[k]$ is defined as follows:

$$f(y) = \sum_{k=0}^{\infty} F[k](y-y_0)^k \tag{24}$$

The DTM has been applied to obtain the solutions of Eq. (1) and Eq. (3).

$$(k+1)(k+2)(k+3)(k+4)u_1[r+4] = \sigma^2(k+1)(k+2)u_1[k+2] +$$

$$2E_1E_3I(\sum_{r=0}^{k}(r+1)u_1[r+1](k-r+1)u_1[k-r+1] + \sum_{r=0}^{k}(r+1)(r+2)u_1[r+2]u_1[k-r]) + \tag{24}$$

$$\frac{E_1E_2}{E_4}\sigma^2\varepsilon\left(\sum_{r=0}^{k}u_1[r]u_1[k-r]\right) + \frac{E_1E_2}{E_4}\varepsilon\sum_{r=0}^{k}(r+1)u_1[r+1](k-r+1)u_1[k-r+1]$$

$$(k+1)(k+2)(k+3)(k+4)u_2[r+4] = \sigma^2(k+1)(k+2)u_2[k+2] +$$

$$2E_1E_3I(\sum_{r=0}^{k}(r+1)u_2[r+1](k-r+1)u_2[k-r+1] + \sum_{r=0}^{k}(r+1)(r+2)u_2[r+2]u_2[k-r]) + \tag{25}$$

$$\frac{E_1E_2}{E_4}\sigma^2\varepsilon\left(\sum_{r=0}^{k}u_2[r]u_2[k-r]\right) + \frac{E_1E_2}{E_4}\varepsilon\sum_{r=0}^{k}(r+1)u_2[r+1](k-r+1)u_2[k-r+1]$$

The initial conditions are as follows

$$u_1[0] = \tau 1, u_1[1] = \tau 2, u_1[2] = \tau 3, u_1[3] = \tau 4, u_2[0] = \tau 5, u_2[1] = \tau 6, u_2[2] = \tau 7, u_2[3] = \tau 8 \tag{26}$$

The constants $\tau 1$, $\tau 2$, $\tau 3$, $\tau 4$, $\tau 5$, $\tau 6$, $\tau 7$, $\tau 8$ numerical values can be find by using the differentially transformed equations then the solutions can be obtain form the system by substituting constants numerical values.

Using non dimensional parameters (6), Eq. (1) and Eq. (3) can be rewrite as

Stream-I

$$\theta_1 = -\frac{1}{\Lambda E_2}\left(48 + \frac{\sigma^2}{E_1}u_1 + \frac{1}{E_1}\frac{d^2 u_1}{dy^2} - I\,E_3\,u_1{}^2\right) \qquad (27)$$

Stream-II

$$\theta_2 = -\frac{1}{\Lambda E_2}\left(48 + \frac{\sigma^2}{E_1}u_2 + \frac{1}{E_1}\frac{d^2 u_2}{dy^2} - I\,E_3\,u_2{}^2\right) \qquad (28)$$

Where θ_1 and θ_2 are the dimensionless temperatures in stream-I and stream-II.

3. Results

The influence of different shapes of nanoparticles on mixed convective nanofluid in a vertical channel saturated with porous media is investigated analytically. The different shapes (namely, non-spherical shapes: Cylinder, Platelet, Brick, and Blade) of nanoparticles are Copper (Cu), Titanium oxide (TiO_2), Silver (AG), Aluminium oxide (Al_2O_3), Ferrous oxide (Fe_3O_4) with the base fluids Water (H_2O) and Ethylene glycol (EG) are considered for the nanofluid. The channel is able to be divided into multiple passages by inserting a thin plate, and it is movable. The flow-governing equations (without inertia) are solved analytically by applying the perturbation method and the - highly nonlinear equations with inertia are solved semi-analytically by applying the differential transform method. The numerical values of profiles obtained by both perturbation and DTM methods agree very well. The flow is depicted pictorially by placing the plate in different positions. The plate is placed in the centre of the channel for Figure 2 to Figure 6, the plate is placed at different places in the channel for Figure 7, and the plate is placed at right wall for other figures. The fixation of parameters is considered for all the graphs except the varying one are $\sigma = 0.5$, $\Lambda = 10$, $\varepsilon = 0.01$, $\phi = 0.02$, $Bi1 = 10$, $Bi2 = 10$, $\delta = 0$, $R_T = 1$, $H_2O - Cu$, $Platelet$.

Figure 2 displays the impact of Λ on the velocity distribution. The enhancement in buoyancy force causes a deficiency in the density of the fluid. Hence, the magnification occurs in the velocity of the flow in both passages. The reverse flow takes place due to the isothermal boundary conditions in the channel with asymmetric wall temperatures [40]. The impact of σ on the velocity profile is depicted in Figure 3. The enhancement in σ causes the magnification in drag force to slow down the velocity of the flow. The impact of ϕ on velocity and temperature cantors is displayed in Figure 4 and 13. The enhancement in ϕ increases the thermal conductivity of the fluid, causing the low viscosity to slow down the velocity and magnify the temperature of the fluid. Figure 5 and Figure 15 display the impact of different nanofluids on velocity and temperature profiles. The optimal velocity and temperature can be seen for water-based silver nanoparticles due to their high thermal conductivity, which causes low viscosity. The influence of different shapes of Cu/H_2O nanoparticles on velocity and temperature profiles is pictorially displayed in Figure 6 and Figure 14. The optimal velocity and temperature are observed for the platelet-shaped nanoparticles, followed by cylinders, blades, and bricks. The increase in densities of nanoparticles depreciates the velocity field. The present result shows that the elongated nanoparticle shapes like platelets and cylinders have lower densities as compared to the square-shaped nanoparticles like blades and bricks. The impact of the baffle plate on the velocity cantor is shown in Figure 7. It is clearly seen that the velocity is very high when the plate is placed near the wall. Fluids can easily flow in the wide passage compared to the narrow

passage. The impact of δ on the velocity and temperature cantor is displayed in Figure 8 and Figure 9. It is observed that the flow depreciates with the increase in δ. The enhancement in quadratic drag force will diminish the velocity of the flow and enhance the temperature of the flow. Figure 10 displays the comparison of the differential transform method and perturbation method for the velocity profile. It is clearly seen in the figure that the values of both the differential transform method and the perturbation method agree very well for small values of the perturbation parameter ε. The impact of Λ and σ on the temperature profile is shown in Figure 11 and Figure 12. The temperature depreciates with the enhancement in Λ and σ. The value of ε increased to 0.5 to see the difference in temperature profiles for Λ, σ and ϕ. The comparison of water-based and EG-based nanofluids for velocity and temperature profiles is shown in Figure 16 and Figure 17. The velocity and temperature of the flow are low for water-based nanofluids due to their high density and low viscosity.

The Nusselt number values are shown in Table 4 for the different values of governing parameters for platelet shaped $H_2O - Fe_3O_4$ nanofluid in a channel with asymmetric wall temperatures $T_2 > T_1$. The rate of heat transfer is diminishing with enhancement in Λ, ϕ, δ and magnifying with the enhancement in σ and ε. The optimum rate of heat transfer occurred for brick shape $H_2O - TiO_2$ nanofluid.
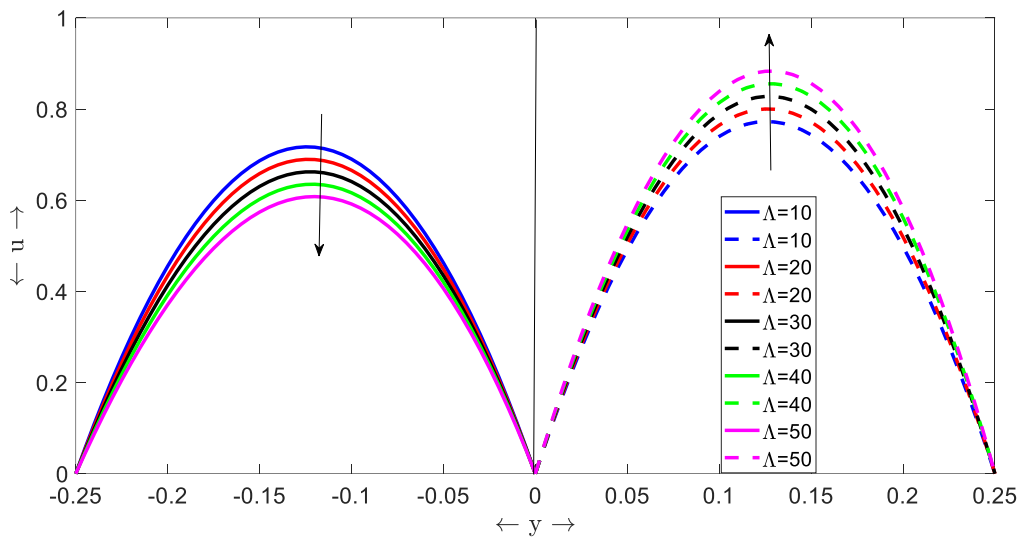
Fig. 2. Velocity contours for Λ
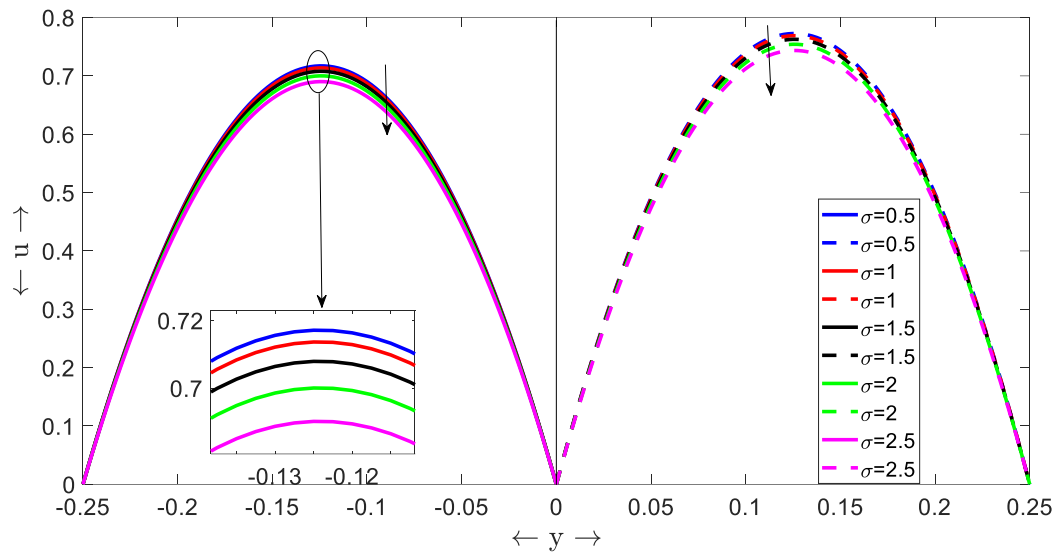
Fig. 3. Velocity contours for σ
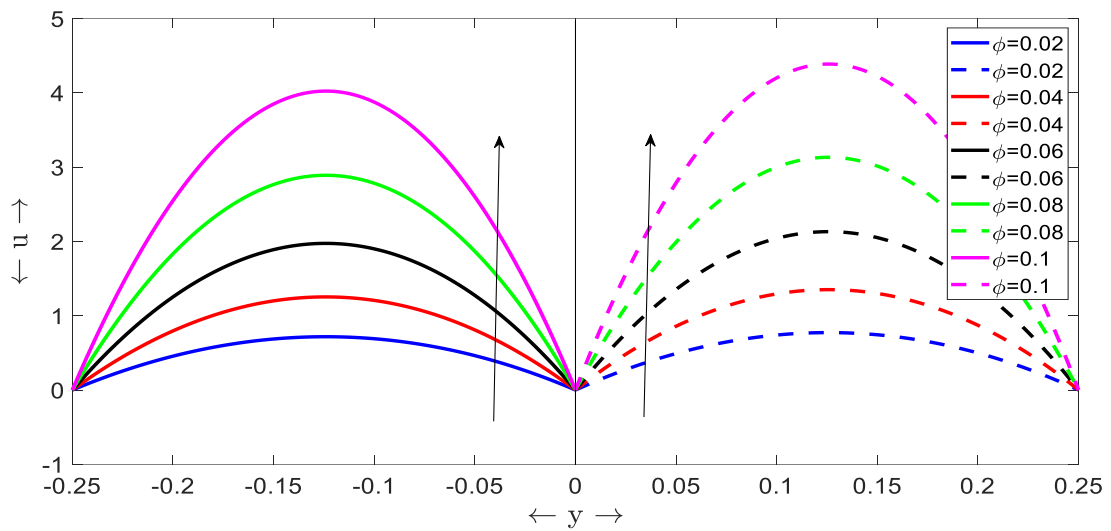
Fig. 4. Velocity contours for ϕ
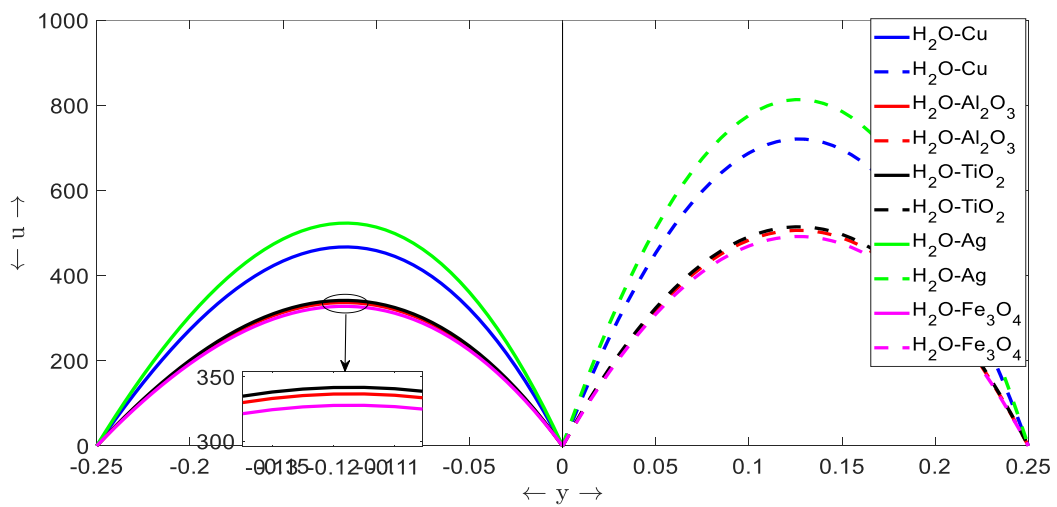
Fig. 5. Velocity contours for different nanofluids
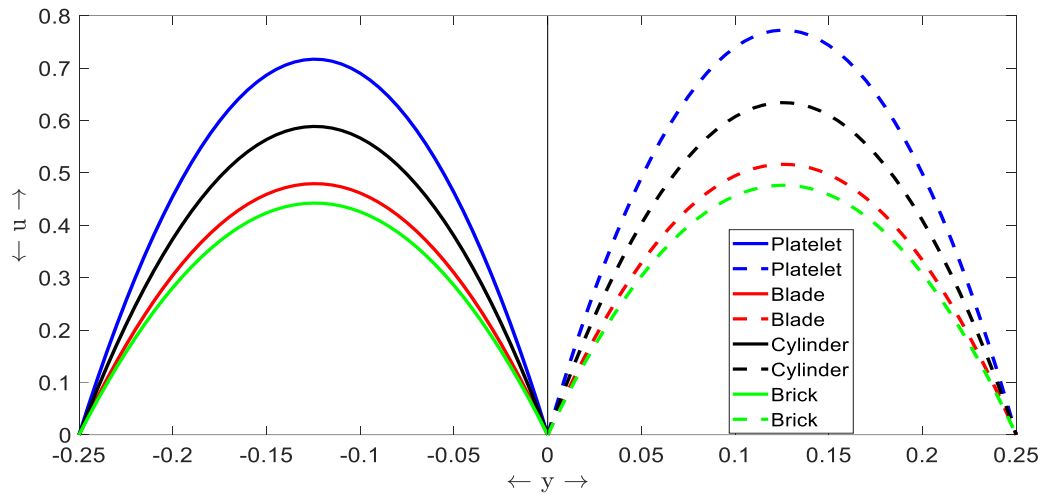
Fig. 6. Velocity contours for different shapes of nanoparticles
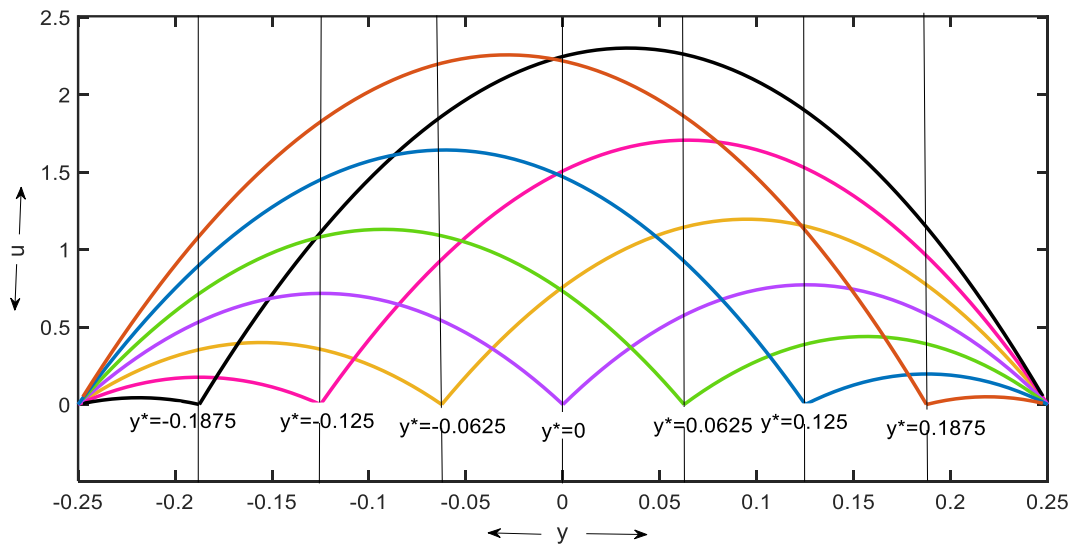
Fig. 7. Velocity contours for different positions of baffle plate
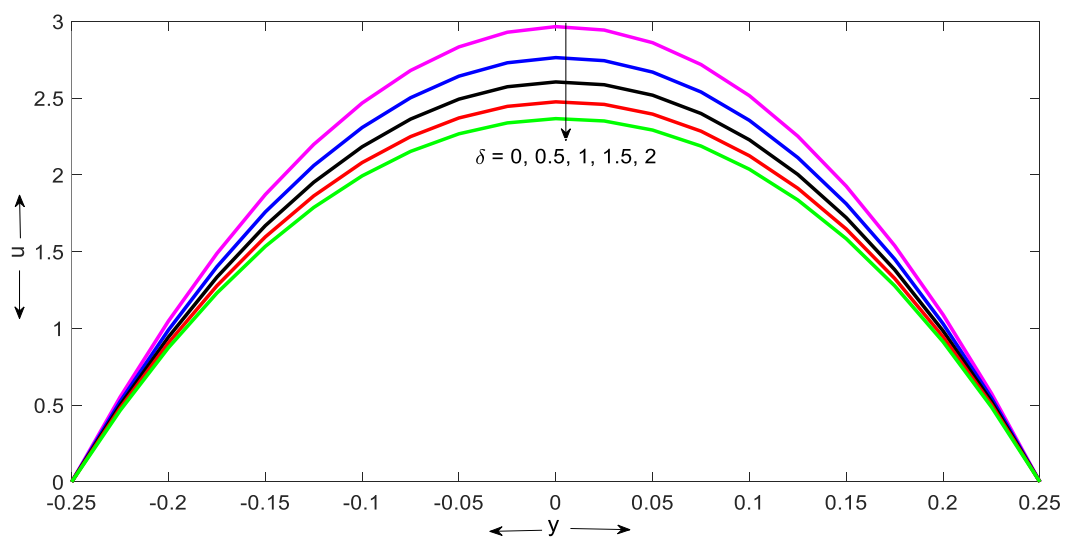
Fig. 8. Velocity contours for δ
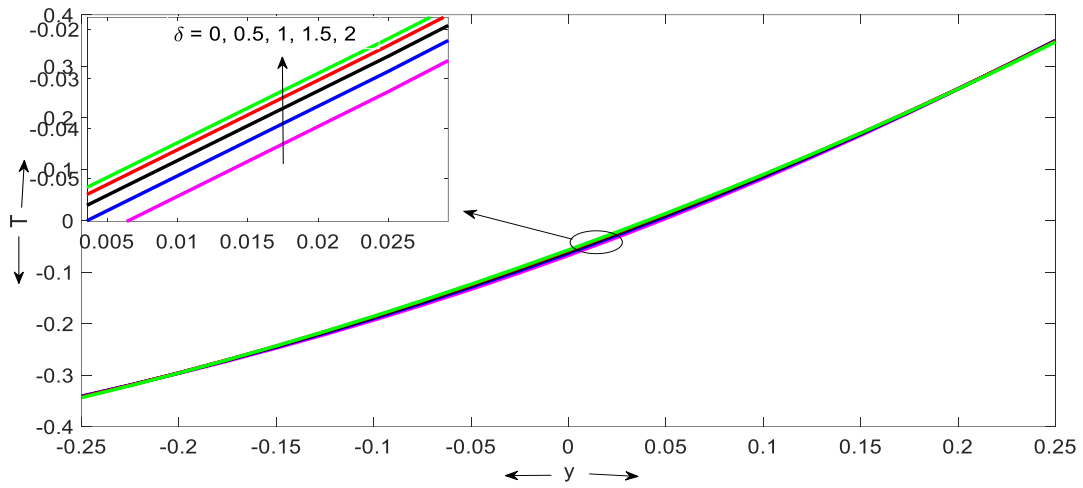
Fig. 9. Temperature contours for δ
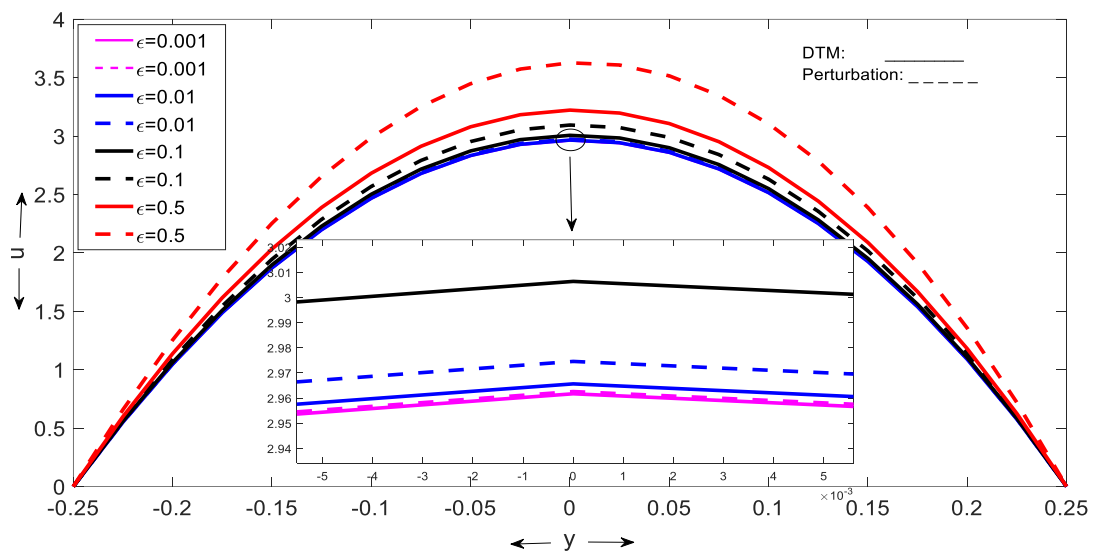
Fig. 10. Velocity comparison with ε
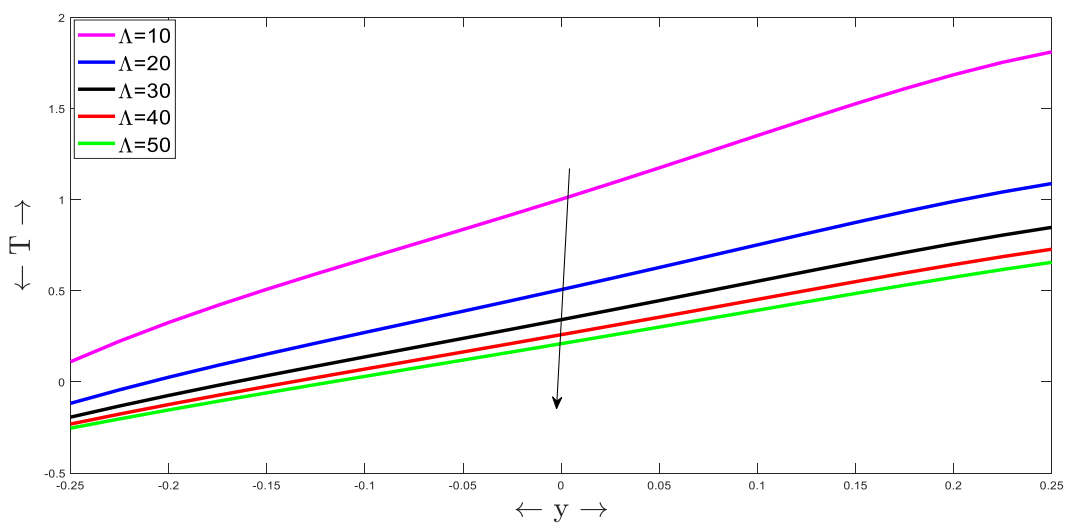
Fig. 11. Temperature contours for Λ
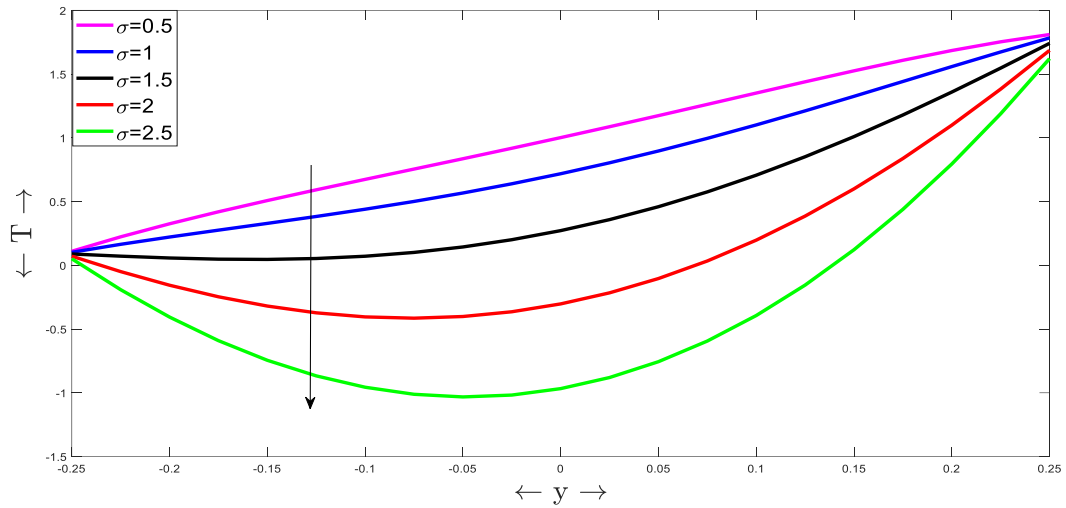
Fig. 12. Temperature contours for σ
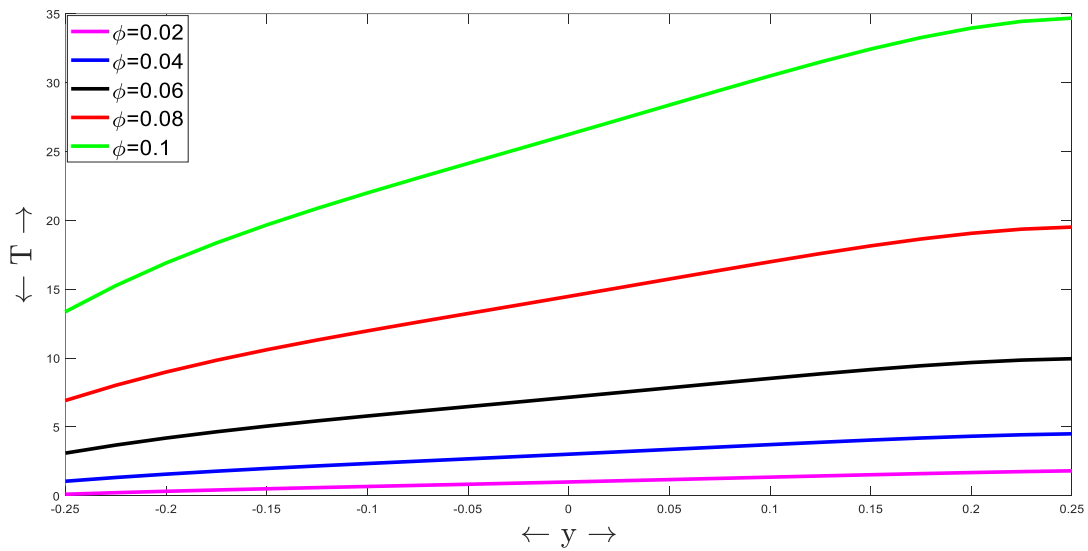
Fig. 13. Temperature contours for ϕ
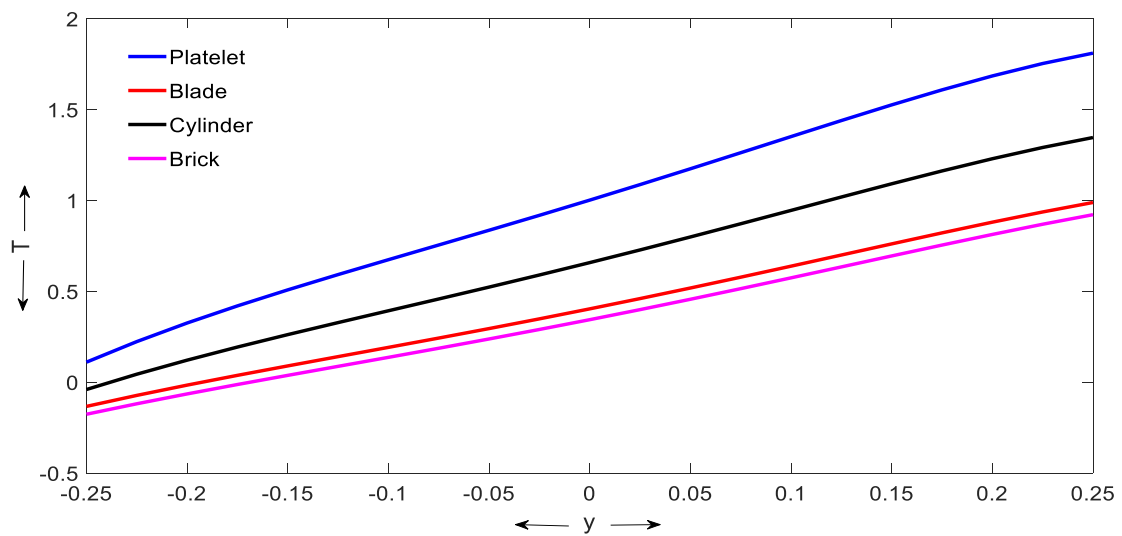
Fig. 14. Temperature contours for different shapes of nanoparticles
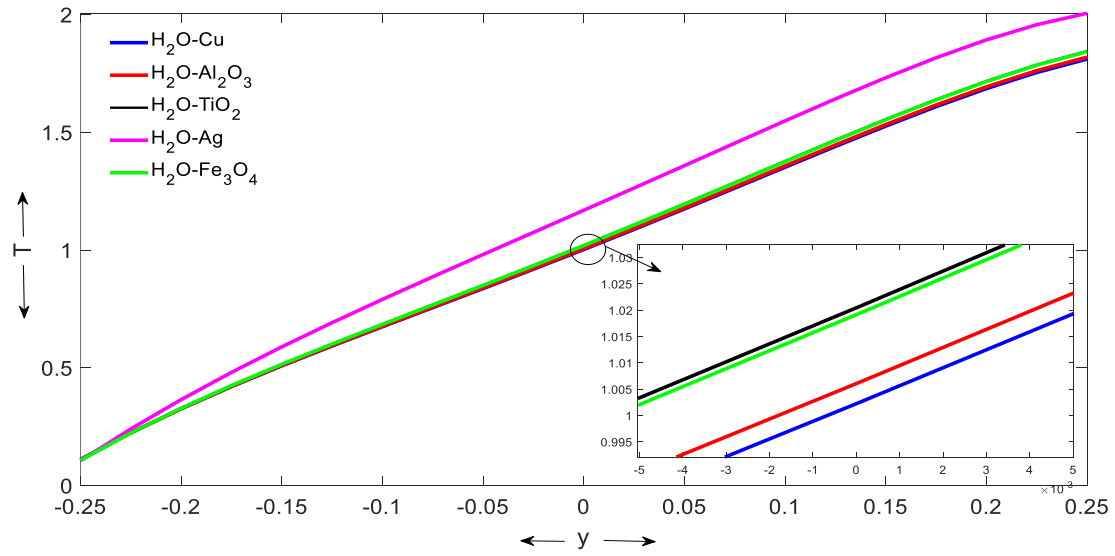
Fig. 15. Temperature contours for different nanofluids
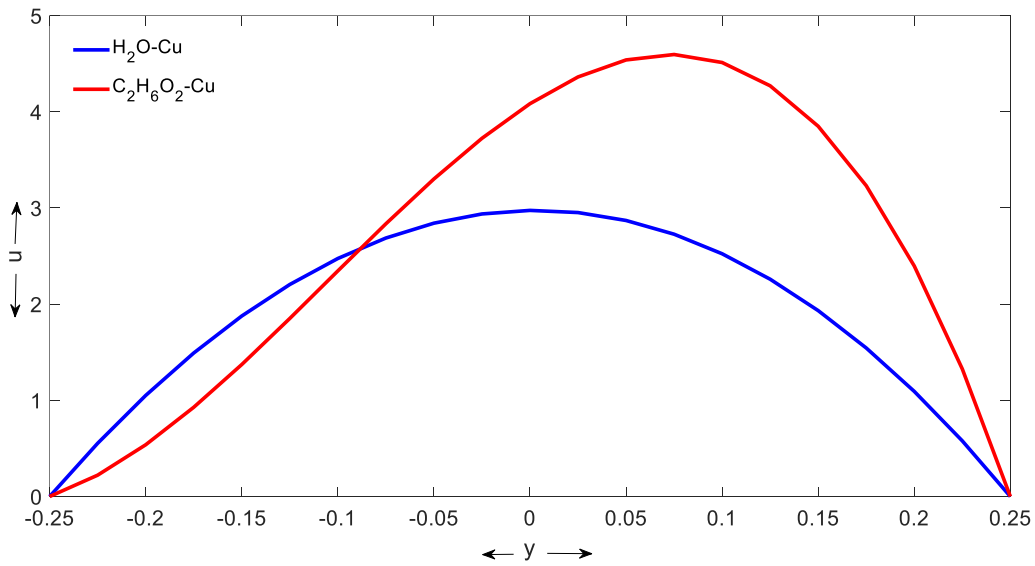
Fig. 16. Velocity comparison for different base-fluids
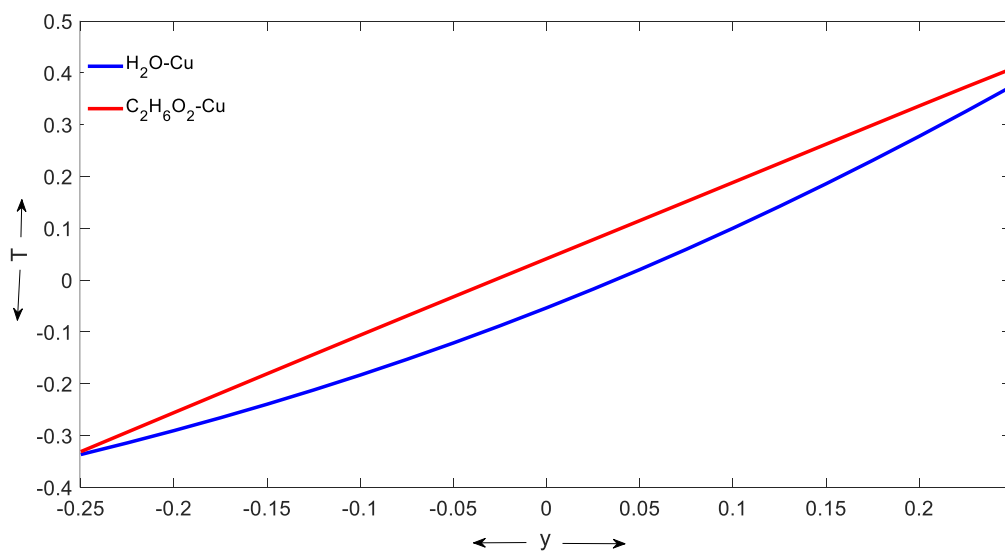
Fig. 17. Temperature comparison for different base-fluids

Table 4
The values of Nusselt numbers for different governing parameters

Λ	σ	ϕ	δ	ε	Nanofluid	Shape	At Y= - 0.25	At Y= 0.25
10							0.8838	2.0174
20							1.1466	1.7134
30							1.2343	1.6121
	0.5						0.8838	2.0174
	1						−0.8664	3.8554
	1.5						−3.6663	6.8003
		0.0					0.8690	2.0403
		0.02					0.8838	2.0174
		0.05					1.0916	1.9871
			0				0.8838	2.0174
			0.5				0.8669	1.9506
			1				0.8844	1.9329
				0.01			0.8838	2.0174
				0.1			1.6205	2.0207
				0.5			4.8950	2.0357
					H_2O-Cu		0.8760	1.9976
					$H_2O - Al_2O_3$		0.8733	2.0077
					H_2O-TiO_2		0.8855	2.0175
					H_2O-Ag		0.8788	1.9948
					$H_2O-Fe_3O_4$		0.8838	2.0174
					$EG-Cu$		1.5087	1.4114
					$EG-Al_2O_3$		1.4214	1.4558
					$EG-TiO_2$		1.4322	1.4527
					$EG-Ag$		1.5482	1.4081
					$EG-Fe_3O_4$		1.4084	1.4741
						Platelet	0.8838	2.0174
						Blade	0.8291	2.0079
						Cylinder	0.8617	2.0212
						Brick	0.8433	2.0266

4. Conclusions

This study investigates the integral thermal conductivity of nanofluid flow with different shapes of nanoparticles under the influence of a quadratic drag force in a porous channel. Inserted a movable, thin, flat plate with negligible thickness to make a double passage channel. The problem is solved using the perturbation method and the differential transform method. The obtained numerical values are agreed very well for small values of the perturbation parameter.

i. The velocity profile diminishes with the enhancement in σ, δ and magnifies with the increase in ε, Λ and ϕ.

ii. The temperature profile magnifies with the enhancement in σ, δ and diminishes with the increase in Λ and ϕ.

iii. The optimum velocity and temperature cantors are found for platelet-shaped water-based silver nanofluid.

iv. The heat transfer rate is diminishes with the enhancement in Λ, ϕ, δ and magnifies with the enhancement in σ and ε.

v. The optimum rate of heat transfer occurred for brick-shaped $H_2O - TiO_2$ nanofluid.

vi. The maximum velocity is found when the plate is near the wall.

References

[1] Choi, S. US, and Jeffrey A. Eastman. *Enhancing thermal conductivity of fluids with nanoparticles*. No. ANL/MSD/CP-84938; CONF-951135-29. Argonne National Lab. (ANL), Argonne, IL (United States), 1995.

[2] Pak, Bock Choon, and Young I. Cho. "Hydrodynamic and heat transfer study of dispersed fluids with submicron metallic oxide particles." *Experimental Heat Transfer an International Journal* 11, no. 2 (1998): 151-170. https://doi.org/10.1080/08916159808946559

[3] Lee, S., SU-S. Choi, S, and Li, and J. A. Eastman. "Measuring thermal conductivity of fluids containing oxide nanoparticles." (1999): 280-289. https://doi.org/10.1115/1.2825978

[4] Ahmadi, Mohammad Hossein, Amin Mirlohi, Mohammad Alhuyi Nazari, and Roghayeh Ghasempour. "A review of thermal conductivity of various nanofluids." *Journal of Molecular Liquids* 265 (2018): 181-188. https://doi.org/10.1016/j.molliq.2018.05.124

[5] Sarviya, R. M., and Veeresh Fuskele. "Review on thermal conductivity of nanofluids." *Materials Today: Proceedings* 4, no. 2 (2017): 4022-4031. https://doi.org/10.1016/j.matpr.2017.02.304

[6] Li, Calvin H., and G. P. Peterson. "The effect of particle size on the effective thermal conductivity of Al2O3-water nanofluids." *Journal of Applied Physics* 101, no. 4 (2007). https://doi.org/10.1063/1.2436472

[7] Hasan, Mushtaq I., Abdul Muhsin A. Rageb Rageb, and Mahmmod Yaghoubi. "Investigation of a counter flow microchannel heat exchanger performance with using nanofluid as a coolant." (2012). https://doi.org/10.4236/jectc.2012.23004

[8] Hasan, Mushtaq I., Abdul Muhsin A. Rageb Rageb, and Mahmmod Yaghoubi. "Investigation of a counter flow microchannel heat exchanger performance with using nanofluid as a coolant." (2012). https://doi.org/10.4236/jectc.2012.23004

[9] Choi, S. U. S., Z. George Zhang, WLockwoodFE Yu, F. E. Lockwood, and E. A. Grulke. "Anomalous thermal conductivity enhancement in nanotube suspensions." *Applied physics letters* 79, no. 14 (2001): 2252-2254. https://doi.org/10.1063/1.1408272

[10] Keblinski, Phillbot, S. R. Phillpot, S. U. S. Choi, and J. A. Eastman. "Mechanisms of heat flow in suspensions of nano-sized particles (nanofluids)." *International journal of heat and mass transfer* 45, no. 4 (2002): 855-863. 10.1016/S0017-9310(01)00175-2

[11] Kim, Jake, Yong Tae Kang, and Chang Kyun Choi. "Analysis of convective instability and heat transfer characteristics of nanofluids." *Physics of fluids* 16, no. 7 (2004): 2395-2401. https://doi.org/10.1063/1.1739247

[12] Buongiorno, Jacopo. "Convective transport in nanofluids." (2006): 240-250. https://doi.org/10.1115/1.2150834

[13] Pil Jang, Seok, and Stephen US Choi. "Effects of various parameters on nanofluid thermal conductivity." (2007): 617-623. https://doi.org/10.1115/1.2712475

[14] Das, Sarit K., Stephen U. Choi, Wenhua Yu, and T. Pradeep. *Nanofluids: science and technology*. John Wiley & Sons, 2007.

[15] Sheikholeslami, M., M. Gorji-Bandpy, D. D. Ganji, Soheil Soleimani, and S. M. Seyyedi. "Natural convection of nanofluids in an enclosure between a circular and a sinusoidal cylinder in the presence of magnetic field." *International Communications in Heat and Mass Transfer* 39, no. 9 (2012): 1435-1443. https://doi.org/10.1016/j.icheatmasstransfer.2012.07.026

[16] Sheikholeslami, M., M. Hatami, and D. D. Ganji. "Analytical investigation of MHD nanofluid flow in a semi-porous channel." *Powder Technology* 246 (2013): 327-336. https://doi.org/10.1016/j.powtec.2013.05.030

[17] Soleimani, Soheil, M. Sheikholeslami, D. D. Ganji, and M. Gorji-Bandpay. "Natural convection heat transfer in a nanofluid filled semi-annulus enclosure." *International Communications in Heat and Mass Transfer* 39, no. 4 (2012): 565-574. https://doi.org/10.1016/j.icheatmasstransfer.2012.01.016

[18] Mintsa, Honorine Angue, Gilles Roy, Cong Tam Nguyen, and Dominique Doucet. "New temperature dependent thermal conductivity data for water-based nanofluids." *International journal of thermal sciences* 48, no. 2 (2009): 363-371. https://doi.org/10.1016/j.ijthermalsci.2008.03.009

[19] Chon, Chan Hee, Kenneth D. Kihm, Shin Pyo Lee, and Stephen US Choi. "Empirical correlation finding the role of temperature and particle size for nanofluid (Al2O3) thermal conductivity enhancement." *Applied physics letters* 87, no. 15 (2005). https://doi.org/10.1063/1.2093936

[20] Akhgar, Alireza, and Davood Toghraie. "An experimental study on the stability and thermal conductivity of water-ethylene glycol/TiO2-MWCNTs hybrid nanofluid: developing a new correlation." *Powder Technology* 338 (2018): 806-818. https://doi.org/10.1016/j.powtec.2018.07.086

[21] Esfe, Mohammd Hemmat, Somchai Wongwises, Ali Naderi, Amin Asadi, Mohammad Reza Safaei, Hadi Rostamian, Mahidzal Dahari, and Arash Karimipour. "Thermal conductivity of Cu/TiO2–water/EG hybrid nanofluid: Experimental data and modeling using artificial neural network and correlation." *International communications in heat and mass transfer* 66 (2015): 100-104. https://doi.org/10.1016/j.icheatmasstransfer.2015.05.014

[22] Yacine, Khelili, Abderrazak Allali, and Rafik Bouakkaz. "Numerical investigation of forced convective heat transfer around a solid circular cylinder utilizing nanofluid in unsteady regime." *Engineering Review: Međunarodni časopis namijenjen publiciranju originalnih istraživanja s aspekta analize konstrukcija, materijala i novih tehnologija u području strojarstva, brodogradnje, temeljnih tehničkih znanosti, elektrotehnike, računarstva i građevinarstva* 39, no. 3 (2019): 261-269. https://doi.org/10.30765/er.39.3.07

[23] Prasad, M. Karuna, S. H. Naveenkumar, C. S. K. Raju, and S. Mamatha Upadhya. "Nonlinear thermal convection on unsteady thin film flow with variable properties." In *Journal of Physics: Conference Series*, vol. 1427, no. 1, p. 012016. IOP Publishing, 2020.

[24] Sajjan, Kiran, N. Ameer Ahammad, C. S. K. Raju, M. Karuna Prasad, Nehad Ali Shah, and Thongchai Botmart. "Study of nonlinear thermal convection of ternary nanofluid within Darcy-Brinkman porous structure with time dependent heat source/sink." *AIMS Mathematics* 8, no. 2 (2023): 4237-4260. https://doi.org/10.3934/math.2023211

[25] Maheswari, Chundru, Mohana Ramana Ravuri, G. Balaji Prakash, D. Ramesh, and D. Vijaya Kumar. "Influence of Thermophoresis and Brownian Motion on MHD Hybrid Nanofluid MgO-Ag/H2O Flow along Moving Slim Needle." *Journal of Advanced Research in Applied Sciences and Engineering Technology* 36, no. 2 (2023): 67-90. https://doi.org/10.37934/araset.36.2.6790

[26] Zainal, Nurul Amira, Najiyah Safwa Khashi'ie, Iskandar Waini, Khairum Hamzah, Sayed Kushairi Sayed Nordin, Abdul Rahman Mohd Kasim, Roslinda Nazar, and Ioan Pop. "Analysis of Solution Stability in Al2O3-Cu/H2O over a Stretching/Shrinking Wedge." *Journal of Advanced Research in Fluid Mechanics and Thermal Sciences* 111, no. 2 (2023): 116-125. https://doi.org/10.37934/arfmts.111.2.116125

[27] John, Clera Peter, Roshafima Rasit Ali, Kamyar Shameli, Zatil Izzah Tarmizi, Mohd Shahrul Nizam Salleh, and Justin Chan Zhe. "Formulation of Titanium Dioxide Nanoparticles Using Sol-gel Technique." *Journal of Research in Nanoscience and Nanotechnology* 4, no. 1 (2021): 35-48. https://doi.org/10.37934/jrnn.4.1.3548

[28] Yeap, Swee Pin, and Mohammad Afiq Afiki Ismail. "Characterization of Surface Morphology and Magnetic Properties of Fe3O4-Deposited Alginate Bead." *Progress in Energy and Environment* (2020): 11-17.

[29] Khan, M. Sabeel. "Heat transfer enhancement of automobile radiator using H2O–CuO nanofluid." *Aip Advances* 7, no. 4 (2017). https://doi.org/10.1063/1.4982669

[30] Khan, Sabeel M., M. Hammad, S. Batool, and H. Kaneez. "Investigation of MHD effects and heat transfer for the upper-convected Maxwell (UCM-M) micropolar fluid with Joule heating and thermal radiation using a hyperbolic heat flux equation." *The European Physical Journal Plus* 132 (2017): 1-12. https://doi.org/10.1140/epjp/i2017-11428-6

[31] Khan, Sabeel M., M. Hammad, and D. A. Sunny. "Chemical reaction, thermal relaxation time and internal material parameter effects on MHD viscoelastic fluid with internal structure using the Cattaneo-Christov heat flux equation." *The European Physical Journal Plus* 132 (2017): 1-11. https://doi.org/10.1140/epjp/i2017-11599-0

[32] Taimoor Dil and Khan, M. Sabeel. "A non-Fourier approach towards the analysis of heat transfer enhancement with water based nanofluids through a channel." *AIP Advances* 8, no. 5 (2018). https://doi.org/10.1063/1.5005870

[33] Khan, Sabeel M., and H. Kaneez. "Numerical computation of heat transfer enhancement through Cosserat hybrid nanofluids using continuous Galerkin–Petrov method." *The European Physical Journal Plus* 135, no. 2 (2020): 1-19. 10.1140/epjp/s13360-020-00226-w

[34] Awang, Noorehan, Nurul Hidayah Ab Raji, Anis Athirah Rahim, Mohd Rijal Ilias, Sharidan Shafie, and Siti Shuhada Ishak. "Nanoparticle Shape Effects of Aligned Magnetohydrodynamics Mixed Convection Flow of Jeffrey Hybrid Nanofluid over a Stretching Vertical Plate." *Journal of Advanced Research in Applied Mechanics* 112, no. 1 (2024): 88-101. https://doi.org/10.37934/aram.112.1.88101 .

[35] Azmi, Nadhira Azreen, Mohd Rijal Ilias, Siti Shuhada Ishak, Roselah Osman, and Abdul Rahman Mohd Kasim. "Maxwell Hybrid Nanofluid Flow Towards a Stagnation Point on a Stretching/Shrinking Inclined Plate with Radiation and Nanoparticles Shapes Effect." *Journal of Advanced Research in Numerical Heat Transfer* 16, no. 1 (2024): 1-16.

[36] Memon, Muhammad Asif, Kavikumar Jacob, Hazoor Bux Lanjwani, Umair Khan, El-Sayed M. Sherif, and Ioan Pop. "Thermal analysis for hydromagnetic flow of Darcy-Forchheimer hybrid nanofluid with velocity and temperature slip effects: Scrutinization of stability and dual solutions." *Advances in Mechanical Engineering* 15, no. 11 (2023): 16878132231209875. https://doi.org/10.1177/16878132231209875

[37] Memon, M. Asif, Mushrifah AS Al-Malki, Muhammad Sabeel Khan, Shafqat Hussain, Haseeb ur Rehman, and Amsalu Fenta. "Squeezed Darcy–Forchheimer Casson nanofluid flow between horizontal plates under the effect of inclined magnetic field." *Nanoscale Advances* 5, no. 24 (2023): 6925-6934. https://doi.org/10.1039/D3NA00769C

[38] Memon, M. Asif, Muhammad Sabeel Khan, S. Saleem, S. M. Eldin, and Kavikumar Jacob. "Heat transfer through a higher grade Forchheimer porous CuO–H2O-nano-medium confined between non-isothermal moving plates." *Case Studies in Thermal Engineering* 47 (2023): 103035. https://doi.org/10.1016/j.csite.2023.103035

[39] Zhou, J. K. "Differential transformation and its applications for electrical circuits." (1986).

[40] Zanchini, Enzo. "Effect of viscous dissipation on mixed convection in a vertical channel with boundary conditions of the third kind." *International Journal of Heat and Mass Transfer* 41, no. 23 (1998): 3949-3959. https://doi.org/10.1016/S0017-9310(98)00114-8

[41] Prathap Kumar, J., J. C. Umavathi, B. J. Gireesha, and M. Karuna Prasad. "Mixed convective flow in a vertical double passage channel filled with nanofluid using Robin boundary conditions." *Journal of Nanofluids* 5, no. 4 (2016): 549-559. https://doi.org/10.1166/jon.2016.1244

[42] Umavathi, Jawali C., Bernardo Buonomo, Oronzio Manca, and Mikhail A. Sheremet. "Heat transfer of chemically reacting mixed convection fluid using convective surface condition: Non-Darcy model." *Thermal Science and Engineering Progress* 25 (2021): 101044. https://doi.org/10.1016/j.tsep.2021.101044

[43] Aaiza, Gul, Ilyas Khan, and Sharidan Shafie. "Energy transfer in mixed convection MHD flow of nanofluid containing different shapes of nanoparticles in a channel filled with saturated porous medium." *Nanoscale research letters* 10 (2015): 1-14. https://doi.org/10.1186/s11671-015-1144-4